SUBMISSION TO ENGINEERING GEOLOGY

DATE:

08/06/2014

TITLE:

"An experimental study on the compaction and collapsible behaviour of a flood defence embankment fill."

AUTHORS:

Gráinne El Mountassir[a], Marcelo Sánchez[b] and Enrique Romero[c]

POSITION & AFFILIATION:

[a] Lecturer, Department of Civil and Environmental Engineering, University of Strathclyde, Glasgow, UK, grainne.elmountassir@strath.ac.uk

[b] Associate Professor, Zachry Department of Civil Engineering, Texas A&M University, College Station, Texas, 77843-3136, USA, msanchez@civil.tamu.edu

[c] Director of Research, Departament d'Enginyeria del Terreny, Cartogràfica i Geofísica, Universitat Politècnica de Catalunya, Barcelona, Spain, enrique.romero-morales@upc.edu

CORRESPONDING AUTHOR:
Dr Marcelo Sánchez
Zachry Department of Civil Engineering
Texas A&M University
College Station Texas
77843-3136, USA
Telephone: (+1) 979 862 6604
Fax: (+1) 979 862 7696
E-mail: msanchez@civil.tamu.edu

ABSTRACT:

With renewed interest in the performance of flood embankments globally, it is important that the performance of fills in conditions similar to 'as-constructed' are scrutinised. The fill material investigated in this study was sampled from flood embankments located along the Bengawan Solo River in East Java, Indonesia. The recurrent history of overtopping and stability issues in these embankments provided the motivation for developing a better understanding of the behaviour of this compacted fill under different loading and wetting conditions. The site investigation revealed that the embankment fill was compacted at low dry densities and that there was local variation in the dry densities determined. A detailed study highlighted that at low compactive efforts this fill material exhibits an irregular double-peak compaction curve, which can be explained by the tendency of this fill to form aggregates on wetting. To cover different plausible operational conditions of these embankments, saturated and unsaturated compression oedometer tests and one-dimensional collapse tests were performed under different initial conditions. Specimens compacted at conditions similar to 'as-constructed' exhibited significant collapse deformation (up to 13.6%) on wetting. Evolution of the microstructure during loading and wetting paths was investigated using MIP and ESEM. A physically-based framework proposed by Romero (2013) was used to explain the changes in the macroscale collapse behaviour observed in the oedometer tests based on the evolution of microporosity. Using this model the evolution of the microporosity with dry density and water content was presented. This microstructural approach could be used as a tool for specifying appropriate compaction conditions for earthworks where fill material is susceptible to volumetric collapse.

KEYWORDS:

flood embankments, laboratory tests, irregular compaction curve, collapse under wetting.

1. Introduction

Flood defence embankments are generally considered to be simple, low cost structures and consequently their construction is often poorly controlled. These factors may contribute to local variation in soil densities within the embankment body and a prevalence of low relative compaction (RC) values, where RC is defined as the ratio between the 'as-compacted' field dry density and the maximum laboratory (Proctor or British Standard) dry density. The performance of embankments may be significantly affected by the presence of fill compacted to low dry densities, because many key properties (e.g. permeability, shear strength and compressibility) are strongly dependent on soil dry density. Furthermore, compacted soils with an open structure (i.e. low dry density) may also be susceptible to volumetric collapse compression upon wetting. This paper focuses on the collapsible behaviour of a fill material used to construct flood defence embankments (i.e. levees) in Indonesia.

Volumetric collapse upon wetting in soils was defined by Lawton et al. (1992) as the densification of a soil caused by the addition of water at a constant total vertical stress (σ_v). This phenomenon requires four main conditions to occur (e.g. Barden et al. 1973; Mitchell 1993): (i) an open partly unstable, partly saturated fabric; (ii) high enough total stress that causes the structure to be metastable; (iii) a cementing agent, including soil suction which stabilises the structure when dry and (iv) the addition of water. The reduction of matric suction upon wetting has been identified as the primary cause of volumetric collapse (e.g. Houston and Houston, 1997). Furthermore, wetting softens aggregates and weakens the binding effect of clay bridges present between aggregates contributing to the phenomenon of volumetric collapse. Flood embankments clearly have a readily available access to water and the fill material may also have an open unsaturated fabric if constructed under dry conditions, particularly at low dry densities.

In this paper the volumetric collapse behaviour of the fill material was investigated using conventional oedometer equipment (e.g. Booth, 1975, 1977; Lawton et al.; 1989, 1992). Tests were carried out on specimens compacted at different initial conditions, which were associated with the variability of dry density and moisture content observed in the field and also on undisturbed specimens. The undisturbed specimens were sampled from the existing embankment fill. The fabric of the Bengawan Solo fill was investigated, before and after volumetric collapse, with the aid of two experimental techniques: Environmental Scanning Electron Microscopy (ESEM) and Mercury Intrusion Porosimetry (MIP). ESEM (or SEM, Scanning Electron Microscopy) and MIP have often been used independently or together in the investigation of microstructural features of soils (e.g. Collins and McGown, 1974; Delage and Lefebvre, 1984; Griffiths and Joshi, 1989; Prapaharan et al., 1991; Al-Mukhtar et al., 1996; Romero et al., 1999; Simms and Yanful, 2001; Cuisinier and Laloui, 2004; Thom et al., 2007; Romero and Simms, 2008) and in the investigation of collapsible soils (e.g. Barden et al., 1973; Prapaharan et al., 1991; Phien-wej et al., 1992; Jommi and Sciotti, 2003; Rao and Revanasiddappa 2003 and 2005).

Studies have shown that the fabric of compacted soils is characterised by a multi-modal pore size distribution, which typically consists of two basic dominant pore levels: inter-aggregate (macropores) pores and the intra-aggregate (micropores)

pores (e.g. Delage et al., 1996; Lloret et al., 2003; Romero and Simms, 2008; Romero et al., 2011). Considering this, the void ratio can thus be similarly separated into the macrostructural void ratio, e_M (volume of macropores/volumes of solids) and the microstructural void ratio, e_m (volume of micropores/ volume of solids) and, such that $e= e_m + e_M$ (e.g. Sánchez et al., 2005). Soil aggregates, when unconfined (particularly those containing an active clay component) swell with increasing moisture content and shrink with reducing moisture content, influencing the ability of the aggregates to store water (Romero et al., 2011). During wetting, water will fill the micropores (intra-aggregate) before water begins to fill the macropores (inter-aggregates). Romero et al. (2011) proposed a physically-based model which relates the evolution of the microvoid ratio, e_m with water ratio ($e_w=w\rho_s/\rho_w$). This microstructural model has been previously used to successfully capture the influence of microstructural effects on water retention behavior, to explain the evolution of compacted microstructure along wetting and drying paths and its influence on hydraulic properties (Romero et al., 2011; Della Vecchia et al., 2013; Romero, 2013).

The microstructural model described above has been used here to study in more detail the effect of compactive effort on fill collapsibility. This approach (i.e. Romero, 2013) has been used to plot in the compaction plane (i.e. water content versus dry density) the microstructure of the Bengawan Solo fill created on compaction at different conditions using MIP data. This is then related to the macroscale volumetric collapse behavior observed in the oedometer tests. The paper also explores the impact of the soil aggregations developed during compaction on the irregular double-peak compaction curve observed in this material.

It is likely that many of the conditions observed along the Bengawan Solo embankments (e.g. variation of dry densities, prevalence of low dry densities, dry of optimum compaction conditions, embankment protection measures) may be found in similar levees, thus the main results and approach outlined in this work could be a useful practical tool for specifying compaction conditions where locally sourced fill material is susceptible to volumetric collapse.

2. Site and fill material

This section presents first a brief description of the Bengawan Solo site, followed by characterisation of the fill material.

2.1 Site

The flood embankment fill investigated here corresponds to a section located along the Bengawan Solo River, in the village of Kedungharjo, East Java, Indonesia (Figure 1). The source of the river lies in the Sewu Mountain Range in Central Java and it enters the sea, north of Surabaya in East Java. The Bengawan Solo River drains a catchment area of almost 20,000 km ; the population within this basis was estimated at over 16 million in 2005 (Hidayat et al., 2008). The Bengawan Solo River is the longest river on the island of Java at 540 km long. At the site in Kedungharjo the Bengawan Solo River is 100m wide and the flood embankment is a 10m high stepped embankment. The water level can vary as much as 10m between the dry and wet season, when the embankments are frequently overtopped. The embankments along the Bengawan Solo River have a history of overtopping and failure, along with extensive erosion of embankment faces (El Mountassir, 2011). In order to protect against erosion a number of remedial measures including rock filled gabion reinforcement (Figure 2) and concrete protection slabs have been introduced.

The weather in this region is typified by the dry and wet monsoon seasons. A consequence of this is that construction of the embankments can only be carried out during the dry season when river levels are low. Furthermore, and as mentioned by Brown (1999), poor access routes in remote rural areas can prevent large construction equipment from reaching sites, resulting in smaller compaction equipment often being used. Additional limitations associated with construction costs can also lead to the use of an unskilled local workforce.

2.2 Site tests and sampling

Figure 3a presents a typical cross-section of the man-made embankments at the village of Kedungharjo; showing the embankment protection (concrete slab in this case), the nearby village and the position of the borehole corresponding to the soil profile presented in Figure 3b. During May 2006 (i.e. at the end of the wet season) a site investigation was carried out along a section of embankment where gabion reinforcement had been constructed to prevent erosion (see Figure 2). Field tests were carried out and samples collected were used in the laboratory tests presented in the following sections.

In-situ dry densities of the fill material were determined using the sand replacement method in accordance with BS1377-9 (BSI, 1990). A marked non-homogeneous distribution of fill densities and water content was observed, with quite a wide range in magnitudes. Dry densities varying from 1.18-1.36Mg/m^3 were determined alongside water contents ranging from 36-43%. The low dry densities measured in the embankment can be explained by considering that this material was compacted in layers of 0.40m using small compaction equipment on the dry side of optimum to 80-85% of standard Proctor maximum dry density (Soemitro, 2006). One week prior to the site visit the embankments were overtopped. The compacted fill has been wetted over time, including during recent overtopping events, which led to the high water contents of the fill when the samples were obtained. Shear vane tests were also carried out and the undrained shear strength obtained ranged from 20-40kPa, indicating a soft soil as classified in BS: 8004 (BSI, 1986).

Disturbed and undisturbed material was sampled from two different depths 0.5m - 1.0m and 1.0 - 1.5m in order to perform the tests presented in the following sections. As for the undisturbed material, block samples were retrieved as described in the Report on Tropical Residual Soils by the Geological Society Engineering Group Working Party (Fookes, 1990).

2.3 Basic soil characterisation

The Bengawan Solo fill is an organic silt of high plasticity; the basic soil properties and classification are given in Table 1 for depths 0.5 - 1.0 m and 1.0 - 1.5m. Figure 4a shows the X-ray diffractograms of random powder samples using the total soil fraction. Non-clay minerals present include quartz, calcite and feldspar (plagioclases); some of the smaller peaks (to the left of Figure 4a) indicate the presence of Montmorillonite and Kaolinite clay minerals. Table 2 presents the mineralogical quantification of the total fraction. The type and quantity of clay minerals present were further investigated by carrying out X-ray diffraction tests on oriented aggregates (e.g. Poppe et al., 2001). Figure 4b presents the X-ray diffractograms of oriented samples in the < 2µm fraction for D2 (0.5 - 1.0m), after three different treatments: (i) sample obtained at room temperature (AO), (ii) after saturating with ethylene glycol (EG), and (iii) after heating to 550°C (550°C). These oriented diffractograms highlight that montmorillonite and kaolinite are the main clay minerals present in this soil with a prevalence of montmorillonite (88 % of the clay fraction) for both depths. This high percentage of montmorillonite explains the high activity values ($A \geq 1$, Table 1).

2.4. Compaction behaviour

The British Standard Heavy (BSH) and Light (BSL) tests were carried out according to BS 1377-4 (BSI, 1990) with an input energy per unit volume of 2682 kJ/m^3 and 596 kJ/m^3 respectively. These energy levels are the same as the modified and standard Proctor tests, respectively. The low dry densities obtained during the site visit (Section 2.2) are related to the low compaction effort applied during the construction of the embankments. To study the compaction behaviour of this soil in the laboratory with compaction efforts more representative of the energy used to construct these embankments, a third compaction level was investigated here. This test was carried out at a lower compaction energy of 132 kJ/m^3 by applying 9 blows of the BS Light 2.5 kg rammer over two layers. This experiment is identified here as the 'Extreme Light' (ExL) test. The ratio between the energy applied in ExL test and the BS Light experiments is equal to the ratio between the BS Light and BS Heavy experiments (i.e. BSH energy/BSL energy = BSL energy/ExL energy).

Figure 5 presents the compaction characteristics of this fill material under these three different compactive efforts. A maximum dry density of 1.47 Mg/m^3 at an optimum water content of 28 % was determined for the BS Light condition. The embankments were constructed at 80-85% of standard Proctor (equivalent to BS Light). This range (i.e. 80-85 %) falls within the Extreme Light compaction curve and explains the low in-situ dry densities determined during the site investigation.

Irregular double-peak compaction curves exist for this material at low compactive efforts (BSL and ExL). This double-peak is removed during compaction at a higher energy level (BSH) where the compaction curve returns to a typical single-peak curve. It is also important to note that in the ExL curve, the first peak (at low moisture content) occurs at a dry density of 1.34Mg/m which is higher than that found at the second peak (1.27Mg/m). In the case of the BSL test the two peaks occur at a similar density. It can also be seen how small variations in moisture content may result in very different dry densities achieved for a specific compactive effort. This is important for explaining the heterogeneous nature of the fill material found on site.

2.5 Soil structure created by compaction

The first step in investigating the soil structure created by compaction was to identify the size and nature of the aggregates created at different moisture contents. All compacted specimens were prepared by spraying water onto the air dried material (passing the 2mm sieve) and handmixing. Each sample was sealed for 48hrs after mixing soil with water. After 48hours no further visible changes to the aggregates formed were observed. As the moisture content is increased the size of the aggregates also increases, (see Figure 6). In order to determine the aggregate size distribution the aggregates created by mixing at 9%, 24% and 36% were then passed through a series of sieves with no addition of dispersant, water or mechanical force. It is evident in Figure 6 that the aggregate size distribution changes with increasing moisture content, from a well-graded distribution for the 9% sample to a fairly uniform distribution for the 36% sample.

The aggregates mixed at 9% range up to 4mm in size, the 24% sample contains aggregates up to 10mm, whereas the 36% sample contains aggregates up to 40mm. It is clear that the size of the aggregates produced is greatly influenced by the mixing moisture content. The very large aggregates observed here at a high moisture content (36%) can be explained by considering that the clay fraction present in this material is montmorillonite and at high moisture contents, smaller aggregations easily attach themselves to each other to form larger and softer overall aggregations (or assemblages).The stiffness and dry density of individual aggregates reduces with increasing moisture content. At a moisture content of 9% the aggregates created are fine, dry, dense and stiff. These aggregates cannot be broken between fingers easily, and are essentially granular in nature. In contrast however are the large, wet, soft aggregates created at 36% moisture content. These aggregates can easily be squeezed between fingers and are plastic in nature. At a moisture content of 24%, the aggregates have increased in size, but remain relatively firm. These changes in the nature of the aggregates are particularly important when considering the structure created by compaction.

These changes can explain the irregular compaction curve obtained for the Bengawan Solo fill at low compactive efforts, observed in Figure 5. The first peak of the irregular compaction curve (Extreme Light compaction curve) occurs at a moisture content of 9%, and can be explained by a packing of these very fine, dry and very dense (granular) aggregates. The second peak of the extreme light curve occurs at a moisture content of 36% and can be explained by its large soft aggregates with low dry density, which easily fuse together under this compactive effort, creating a more homogeneous fabric. The trough (or valley) of the extreme light compaction curve occurs at a moisture content of 22-24% and is a result of the medium sized firm aggregates at intermediate dry density created at this moisture content, which retain their aggregate form under this compactive effort, resulting in an open fabric being created. At this moisture content the stiffness of these aggregates has provided sufficient resistance to the compactive effort, such that the form of the aggregates has been maintained, this was observed consistently in the laboratory. Based on these compaction curves a number of different specimens were prepared in order to study their one-dimensional compression and collapse behaviour on wetting, as explained in the next section.

3. Compression and volumetric collapse behaviour

Oedometer tests were performed on specimens of the Bengawan Solo fill material prepared at different initial conditions of dry density (ρ_{do}) and water content (w_o).

Five series of oedometer tests comprising loading and wetting stages are presented herein, four of them were carried out on remoulded and compacted specimens in the laboratory; and one series was carried out on undisturbed specimens. Compacted specimens were prepared by compacting the fill into the oedometer rings in three layers using a tamping rod, and a small light hammer; the number of blows varied depending on the target dry density. After the addition of each layer the soil was scarified to ensure good contact was made with the above layer. The initial conditions of the different series are plotted in Figure 5 and are as follows:

- Series A: specimens were compacted dry of optimum (average w_o = 19.8%) and at a low dry density (average ρ_{do} = 1.17 Mg/m^3); close to the lowest dry density measured in the field with RC ~ 80% of BSL (Point A Figure 5). This series corresponds to the 'as-constructed' conditions of the embankment during the dry season after loading to field stress levels in the oedometer, for fill material at 4.5m below the crest of the man-made embankment this corresponds to 62kPa. Where protection measures have been installed stress levels are higher.

- Series B: specimens were compacted at dry of optimum (average w_o = 19.4%) at a higher dry density, (average ρ_{do} = 1.37 Mg/m^3); similar to the highest dry density measured in the field with RC ~ 93% of BSL (Point B Figure 5).

- Series C: specimens were compacted close to optimum conditions of the BS Light compaction test (average w_o = 29.2%, average ρ_{do} = 1.43 Mg/m^3), RC > 97 % of BSL (Point C Figure 5).

- Series D: specimens were compacted at the optimum water content of the ExL test (average w_o = 35.9 %) and at a low dry density (average ρ_{do} = 1.18 Mg/m^3, equal to the lowest dry density measured in the field), with RC ~ 80% of BSL (Point D Figure 5).

- Series U: undisturbed specimens were prepared from block samples and had an average w_o = 34.8%, average ρ_{do} = 1.21 Mg/m^3, highlighting the low dry density and high water contents characterising this fill material in the wet season (Point U Figure 5). Distinct variation in the dry density of the undisturbed specimens was found with values ranging from 1.12 to 1.27 Mg/m^3.

The different initial conditions associated with each series are summarised in Table 3. For each series, at least one saturated (prior to loading) compression test, one unsaturated (i.e. constant water content) compression test and a one-dimensional collapse test was carried out.

Figure 7 presents the results of the oedometer tests in Series A. For the specimen saturated prior to loading (under a nominal load of 3kPa) swelling was observed. For the one-dimensional collapse tests (loaded under unsaturated conditions and then subjected to wetting) collapse strains were exhibited which essentially brought the specimens from the unsaturated compression curve to the saturated (prior to loading) compression curve. Other researchers have also found that collapsible soils do not exhibit significant path dependency when loaded and wetted over stress levels observed for typical geotechnical applications (Houston and Houston, 1997; Delage et al., 1995). As the vertical stress applied increased the collapse deformation (i.e. volume change on wetting) observed increased to a maximum of 13.6% at a vertical stress of 125kPa (Figure 7b). Beyond 125kPa increasing stress increases the compression under unsaturated loading conditions and thus acts to reduce collapse deformation (Figure 7b). Figure 7 illustrates that under 'as-constructed' conditions this fill material is susceptible to collapse when subjected to wetting after loading and to display a maximum peak of collapse. It is worth mentioning that the stress level associated with the maximum collapse for the soils of the Series A (i.e. σ_v = 125kPa), may be different for the other series. Nevertheless, for all the collapse tests carried out in this study the samples were wetted at a σ_v = 125kPa. This was done to maintain a common reference load for all the analyses.

For Series B, at a higher compacted dry density (ρ_d =1.37Mg/m) volumetric collapse was still observed (Figure 8a), but significantly less than in Series A (collapse deformation of 2.3% at a vertical stress of 125kPa). In Series C (Figure 8b), as expected, at close to optimum BSL and nearly saturated conditions essentially no collapse was observed on wetting at 125kPa. In Series D at high degree of saturation (Figure 9a) no collapse was observed. Finally, the potential for collapse in undisturbed specimens was investigated in Series U. It should be noted however that when the in-situ sampling took place, the embankments had been recently overtopped, which explains their high initial moisture content (approx. 35%). No collapse was observed in these nearly saturated specimens. Volumetric collapse is an irreversible process and it is likely that several past wetting events contributed to the volumetric collapse of this fill material in-situ. These tests illustrate how increasing the initial dry density of the soil and/or the moisture content can reduce collapse deformation significantly. This is discussed further in Section 6.

4. Microstructural Study

The MIP tests were performed with an Autopore IV 9500 porosimeter; which can reach a maximum pressure of 220MPa (corresponding to a minimum entrance pore diameter of approximately 7nm). MIP is based on the principle that a non-wetting fluid (mercury) will enter the pores of a soil progressively under an applied pressure. Details about this technique can be found elsewhere (e.g. Romero et al., 1999; Delage and Lefebvre 1984; Griffiths and Joshi 1989; Romero and Simms 2008). The ESEM study was done by means of an electroscan 2020 environmental electron microscope.

4.1 Microstructural specimens

The compaction conditions of Series A (dry of optimum and low dry density), were selected for further investigation in the fabric study. The specimens investigated corresponded to the path followed when loading to a vertical stress of 125kPa followed by wetting (i.e. the maximum collapse observed for Series A). As such three different specimens were prepared (Figure 10): (A5-0) compacted; (A5-1) compacted & loaded and (A5-2) compacted, loaded & collapsed. Furthermore a compacted specimen from Series D and an undisturbed specimen from Series U were also investigated for comparison purposes. Details of the preparation and conditions of all five specimens are provided in Table 4.

4.2 MIP Results

MIP is a useful technique for investigating the effect of the volumetric collapse on soil fabric because it enables the quantification of the volume changes at different pore levels. It has however some limitations associated with the range of pores sizes that can be measured. In the upper range, the presence of large inter-aggregate pores (i.e. >450μm) in the specimen cannot be detected. The void ratio (i.e. volume of void/ volume of solid) associated with these non-detected pores is identified hereafter as 'e_{nd}'. In the lower range, there are voids which cannot be intruded due to: (i) the specimen having pores less than 7nm in size (the minimum pore size which can be intruded according to the maximum pressure capacity of the porosimeter used, 223MPa), or (ii) the presence of totally isolated pores. The void ratio related to these non-intruded pores is identified herein as 'e_{ni}' and the void ratio of the specimen intruded by mercury is identified as 'e_{int}'. The total measured void ratio 'e' of the specimen is thus obtained as:

$$e = e_{\mathrm{int}} + e_{nd} + e_{ni} \tag{1}$$

The non-intruded void ratio was estimated by carrying out a MIP test on a desiccated slurry specimen (Figure 11). This specimen was prepared by first creating a slurry at a moisture content of 70%, and then allowing it to shrink freely until air dried. No cracks appeared during the shrinkage stage and the final sample conditions were: w = 9.2%; ρ_d = 2.00Mg/m ; and e = 0.361. This high density specimen displayed no visible inter-aggregates higher than >450μm, thus nil non-detected void ratio (e_{nd} = 0). From Figure 13 the intruded void ratio was determined (e_{int} = 0.283) and using equation (1) the non-detected void ratio was calculated as e_{nd} = 0.078. Given that the non-intruded void ratio relates to micropores < 7nm, and isolated pores, this void ratio is unlikely to vary greatly for different specimens of the same soil. Therefore, it is assumed here that the non-intruded void ratio is the same for all specimens of the Bengawan Solo fill which were investigated using the same MIP equipment.

Figure 12 presents the cumulative void ratio intrusion and pore density function plots for the three specimens A5-0, A5-1 and A5-2. From Figure 12b it can be inferred that the compacted sample (A5-0) has a bi-modal pore size distribution, but one of the pore modes, corresponding to very large inter-aggregate pores, could not be detected in the MIP, as they have a dominant pore size > 450μm. The presence of these very large inter-aggregate pores indicates the very open structure created during compaction at low dry density and dry of optimum moisture content.

Loading the compacted specimen to 125kPa under constant water content conditions resulted in a shift in the inter-aggregate pore size to 170μm, into the range detectable using MIP. Moving from the compacted & loaded (A5-1) to the compacted, loaded & collapsed specimen (A5-2) resulted in a substantial reduction in the dominant pore size observed from 170μm to 2μm. Evidence of these pore sizes found in the corresponding specimens are presented in Figures 12c, d & e.

Given that inter-aggregate pores are by their definition always equal to or larger than intra-aggregate pores, there exists therefore a delimiting pore size which is both an upper bound for the size of intra-aggregate pores and equally a lower bound for inter-aggregate pores within a compacted soil (Romero et al., 2011). Romero et al., (2011) demonstrated that this delimiting pore size can be determined from the dominant peak of compacted specimens subjected to wetting under constant volume, where both the swelling of aggregates is promoted and inter-aggregate porosity is reduced simultaneously. In fact, it was also demonstrated that the same delimiting value is observed for compacted specimens that are subsequently saturated, regardless of mechanical loading conditions.

The dashed line indicated on Figure 12 is thus the delimiting pore size separating the intra-aggregate pores from the inter-aggregate pores. Therefore the dominant peak observed at 2μm for A5-2 can be partially assigned to intra-aggregate pores and partially to the inter-aggregate pores. The shift in pore size between A5-1 and A5-2 due to wetting at constant stress can therefore be interpreted as a result of both the reduction of inter-aggregate pores (macropores) due to collapse and the expansion of intra-aggregates pores (micropores) due to the swelling of aggregates on wetting.

Figure 13 presents the pore size density function plots for A5-2 (compacted loaded & collapsed: w = 27.7%, ρ_d = 1.39Mg/m^3), D (specimen compacted at w = 36.5%, ρ_d = 1.17Mg/m^3) and U (undisturbed specimen: w = 34.7%, ρ_d = 1.36Mg/m^3). It is evident that specimen A5-2 which exhibited volumetric collapse on loading and wetting in the laboratory and specimen U (undisturbed) have very similar microstructure with both samples exhibiting a dominant peak at a pore size of 2μm (see Figures 13b and c). Specimen D also exhibits the same peak in the pore size density function plot at 2μm. However it should be noted that the non-detected void ratio was significant for D (e_{nd} =0.376) indicating that for these compaction conditions there exists an additional porosity which has not been detected as it is greater than 450μm (out with the range of the MIP). Nevertheless at this high moisture content (36.5%) it appears that the aggregates have already reached full swelling giving rise to the same delimiting value between inter-aggregate and intra-aggregate pores of 2μm as observed for A5-2 and U specimens.

4.3 ESEM Results

Figure 14a presents an image of the compacted (A5-0) specimen, which shows an open structure characterised by large inter-aggregate pores (1), surrounded by defined aggregates (2) which are connected via clay bridges (3). It is difficult to discern individual sand grains and silt particles as it appears that everything is clothed with clay particles forming aggregations. Moving to the compacted, loaded (A5-1) specimen in Figure 14b, inter-aggregate pores (4) and defined soil aggregations (5) are still present along with bridging connections (6). However, the loading process may be responsible for breaking some bridging connections, especially those that are brittle in nature. Figure 14c shows the compacted, loaded and collapsed specimen (A5-2). Inter-aggregate pores are less readily visible in the collapsed specimen (Figure 14c), compared to Figure 14a and Figure 14b. It is still possible to detect where soil aggregations existed prior to wetting (7), though these are no longer well defined. Similar changes in fabric due to loading and wetting have been observed using ESEM by Monroy et al. (2010) and Romero et al. (2011).

As a result of wetting, the aggregates become softened (Figure 14c) enabling their rearrangement but also the aggregates themselves swell on wetting, invading the inter-aggregate pores. Both of these phenomena contribute to the loss of inter-aggregate porosity on wetting observed between A5-1 and A5-2 from the MIP results (Figure 12b), which is responsible for the global volume changes observed in the oedometer tests presented in Section 3.

Finally the microstructure of an undisturbed specimen was also investigated using ESEM. There are distinct similarities between the undisturbed specimen (Figure 14d and the A5-2 specimen in Figure 14c, namely both show fused aggregations (7, 8) and visibly less inter-aggregate pores than in A5-0 and A5-1 specimens. The comparison of Figures 14c and 14d suggests that the microstructure of the undisturbed sample is very similar to that of the A5-2 Compacted Loaded & collapsed specimen created in the laboratory with initial conditions, dry of optimum at low dry density, as expected.

5. Discussion

The mechanical study presented in Section 3 has identified that the Bengawan Solo fill material is a collapsible material under dry of optimum and low dry density conditions (Series A). These are quite common conditions in these embankments, where fill material is compacted in layers of 40 cm using light compaction plant and on the dry side of optimum (Soemitro, 2006). This is because (as explained in Section 2), the construction and repair of these embankments takes place during the dry season and limited resources are allocated towards controlling the compaction conditions of the fill material. In fact, quite low dry densities (RC=80%) were measured during the site investigation (Section 2). Therefore, Series A conditions are similar to the 'as-constructed' conditions. The results of Series A are important because they indicate that close to these (as-constructed) conditions the fill material exhibits significant volumetric collapse upon wetting.

To account for the variability in dry densities observed in the site (and also observed in the undisturbed samples), Series B tests were performed close to the highest dry density observed in-situ (around 1.37 Mg/m) and on the dry side (i.e. w = 24%). These samples also exhibited volumetric collapse but to a lesser degree. These tests illustrate how increasing the initial dry density of the soil can considerably reduce the potential for collapse. The increase in dry density of between 15 and 20%, led to a reduction in the collapse deformation on wetting of around 80%. The specification and control of appropriate compaction conditions for fill material which is susceptible to volumetric collapse is one method of minimising unwanted settlements in construction projects, where such settlements may lead to further damage or reduce the functional performance of an earth structure.

It is evident from the microstructural investigation in Section 4 that the soil microstructure undergoes significant evolution during loading and wetting for specimens compacted at low dry density and low water content (Series A), with a shift in the dominant pore size of 170μm to 2μm on wetting (Figure 12). Specimens prepared also at low dry densities, but higher water contents (e.g. Series D) exhibited essentially no volumetric collapse upon wetting. Both of these specimens (i.e. dry of optimum or wet of optimum) present practically the same total void ratio, but their collapsible behaviour is quite different which is due to the differences in the specimen structure arising due to compaction at different water contents.

The investigation of compaction behaviour (Sections 2.4) demonstrated that the Bengawan Solo fill material has an irregular double-peak compaction curve at low compactive effort (Figure 5). Irregular compaction curves have been presented in the literature by many authors (e.g. Olson, 1963; Lee, 1976; Ellis, 1980; Nawari and Schetelig, 1991). Olson (1963) proposed that the double-peak curve would only occur in soils with a dominant percentage of plate shaped particles. The Bengawan Solo fill material however has only a small fraction of clay particles (~15%), albeit this is largely composed of montmorillonite. Lee and Suedkamp (1972) researched the characteristics of irregularly shaped compaction curves by investigating 34 different soils. They found that typically soils with a liquid limit of between 30 and 70% yielded single peak compaction curves, whereas soils with a liquid limit lower than 30% or greater than 70% usually produced irregularly shaped curves. There were a few exceptions to this rule caused by the mineralogy of the soils. The liquid limit of the Bengawan Solo fill material is 53-54% which suggests again that it is the mineralogy of this material which has an influence on its compaction behaviour.

It is proposed here that it is the nature of the aggregates formed at different moisture contents which are responsible for the irregular double-peak compaction curves. At dry moisture contents smaller stiff and very dense aggregates were formed and as moisture content increased larger aggregates were formed on mixing with water. However at higher moisture contents these large and low-density aggregates are softer and fuse together more easily under compactive effort. Such an irregular compaction curve could lead to large variations in dry density with small variations in moisture content, which may be important particularly where flood embankment construction is poorly controlled.

To better understand the microstructure created on compaction at different initial conditions we can use the model developed by Romero et al., (2011) for the evolution of the microvoid ratio with water ratio ($e_w = w\rho_s/\rho_w$) for $e_w \geq e^*_m$:

$$e_m = e^*_m + \beta \left\langle e_w - e^*_m \right\rangle \tag{2}$$

where e^*_m corresponds to a water ratio where the micropores (intra-aggregate) are fully saturated and the macropores (inter-aggregate) are empty of water. $B<1$ is a parameter that describes the tendency of the aggregates to swell under saturated conditions. Figure 15 presents the evolution of e_m with e_w. Data points were determined for the Bengawan Solo fill from MIP data using the criteria outlined in Romero et al., (2011) for delimiting intra-aggregate and inter-aggregate porosity. For specimens compacted dry of optimum with two distinct pore levels, the delimiting pore size, i.e. that which is an upper bound for the intra-aggregate porosity and a lower bound for the inter-aggregate porosity is the depression between the two peaks. For compacted specimens, which have been saturated, the delimiting pore size is the dominant peak of the pore size distribution function determined by MIP. Figure 15 presents the evolution of microstructural void ratio with water ratio using the MIP data presented in Figures 12 and 13. Values of e^*_m = 0.37 and β=0.45 were determined. Values of e^*_m and β for a range of different soils are given in Romero (2013).

Figure 16 presents contours of e_m/e which indicate the contribution of microporosity to total void ratio for the Bengawan Solo fill, plotted on the compaction plane (dry density versus water content). The collapse deformation (i.e. change in volume on wetting) is noted in brackets for specimens compacted at different water contents and initial dry densities, which were wetted at a vertical stress of 125kPa. For low water contents (i.e. w <25%) at low dry densities (80-85% RC), e_m/e is low. For values of e_m/e between 0.3 and 0.4 considerable volumetric collapse occurs if additional loading is applied. As e_m/e increases (0.4 to 0.5) the volume change observed on saturation at 125kPa decreases. Above e_m/e =0.5 no volumetric collapse was observed. This can be explained by considering that as e_m/e increases the intra-aggregate porosity increases and thus the component of porosity due to inter-aggregate pores decreases. Above e_m/e =0.5, the dominant porosity becomes the intra-aggregate porosity and as such the potential for collapse which is associated with inter-aggregate porosity has now been removed.

For high water contents (i.e. w >35%) for the same range of low dry densities, e_m/e remains above 0.5, which explains why no collapse was observed for Series D. The additional loading (125kPa) does not contribute to volumetric collapse in this case. This has important practical implications. For the Bengawan Solo fill, if the material is going to be emplaced at very low dry densities, (80% RC), then the moisture content at which it is emplaced must be high to ensure that significant volumetric collapse does not occur. This is of particular importance for fill materials used in flood embankments, which are subjected to wetting and also may be subjected to additional loading in the form of surface protection as was the case for the Bengawan Solo embankments. This microstructural approach could be used as a tool for specifying appropriate compaction conditions for earthworks where fill material is susceptible to volumetric collapse.

6. Conclusions

This study investigated the behaviour of fill material from flood embankments along the Bengawan Solo River in East Java, Indonesia, under different compaction conditions. Local variation of dry density was observed both during the site investigation (ranging from 1.18 to 1.36Mg/m^3), and in the undisturbed block samples (dry densities between 1.12 to 1.27 Mg/m^3). A detailed study of the compaction behaviour showed that the soil structure formed during compaction strongly depends on the amount of mixing water. The water content affects the size of the aggregates, as well as their dry density and stiffness. As a result the soil aggregations formed at different moisture contents have a significant influence on the final soil dry density achieved for a given compactive effort.

Close to as-constructed conditions (dry of optimum and RC=80%) the Bengawan Solo fill exhibited significant collapse compression behaviour at a range of vertical stresses (from 32kPa to 538kPa); with a maximum collapse at an intermediate stress level (125kPa). The collapse deformation was found to reduce significantly in samples compacted at a higher dry density (RC=93%), albeit still under dry of optimum conditions. Specimens prepared at optimum or wet of optimum moisture content conditions were generally not found to be sensitive to the addition of water, with no collapse observed. This was also the case for specimens compacted at low dry densities (i.e. RC=80%) at optimum or wet of optimum moisture contents.

MIP tests were conducted to investigate the evolution in the pore size distribution during compression and volumetric collapse upon wetting. The volumetric compression after wetting induced a significant reduction of the dominant pore size, with global rearrangement of aggregates contributing to a reduction in the size of inter-aggregate pores and the swelling of aggregates resulting in the expansion of intra-aggregate pores. With the MIP tests it was also possible to detect that essentially all the large macropores (>450 μm) present in the aggregated structure developed during compaction on the dry side, disappeared after wetting. Images obtained using ESEM showed that the wetting of (dry of optimum) compacted specimens resulted in the softening of aggregations, leading to a fused uniform fabric.

A physically-based framework recently proposed by Romero et al. (2011) was used in this paper to interpret the behaviour of the embankment fill observed in the microscopic and macroscopic experiments. By using this model it was possible to present in the compaction plane (i.e water content versus dry density) the evolution of the microporosity with dry density and water content. This plot was then used to explain the collapse behaviour observed across the specimens compacted at different conditions. This microstructural approach could be a useful tool for engineers dealing with collapsible materials.

Acknowledgements

The authors would like to thank the staff and postgraduate students at UPC, Barcelona for their assistance in carrying out the microstructural study (with special thanks to Ms. Alice Lima). In particular, the authors would like to thank Dr. Ana María Fernández Díaz from the CIEMAT Laboratory, Madrid, Spain for carrying out the X-ray diffraction investigation. The support of Dr. Ria Soemitro and Prof. Mark Dyer during the initial stages of this research is also appreciated. The authors gratefully acknowledge the support of the Carnegie Trust, Bellahouston Travelling Scholarship, the Research Enhancement Group at the University of Strathclyde and the EC (contract number MIF1-CT-2006-040375).

References

Al-Mukhtar, M. Belanteur, N. Tessier D. & Vanapalli, S.K. (1996). The fabric of clay soil under controlled mechanical and hydraulic stresses. Applied Clay Science, 11(2-4): 99-115.

Barden, L., McGown, A., Collins K., 1973. The collapse mechanism in partly saturated soil. Engineering Geology 7, 49-60.

Booth, A. R. 1975. The factors influencing collapse settlement in compacted soils. Proceedings of 6th Regional Conference for Africa on Soil Mechanics & Foundation Engineering, Vol. 1, Durban, South Africa. A. A. Balkema, 57-63.

Booth, A.R., 1977. Collapse settlements in compacted soils. Council for Scientific and Industrial Research, Pretoria, South Africa, CSIR Res. Report 324, pp. 1-34.

Brown, R. L., 1999. Vientiane plain flood protection: urgent phase..... Flood Management and Mitigation in the Mekong River Basin, Proceedings of the regional workshop, number 1999/14., Vientiane, LAO PDR,. RAP Publication.

BSI, 1986. Code of practice for Foundations. British Standards, Milton Keynes, 1986, BS 8004.

BSI, 1990. Methods of tests for soils for civil engineering purposes. British Standards, Milton Keynes, 1990, BS 1377: Part 4: Compaction-related tests.

Collins, K., and McGown, A., 1974. The form and function of microfabric features in a variety of natural soils. Géotechnique 24 (2), 223–254.

Cuisinier, O., & Laloui, L., 2004. Fabric evolution during hydromechanical loading of a compacted silt. Int. J. Numer. Anal. Meth. Geomech., 28(6): 483-499.

Delage, P., Audiguier, M., Cui, Y., and Howatt, M.D., 1996. Microstructure of a compacted silt. Can Geotech J; 33: 150-158.

Delage, P., Lefebvre, G., 1984. Study of the structure of a sensitive Champlain clay and of its evolution during consolidation. Canadian Geotechnical Journal 21, 21–35.

Della Vecchia, G., Jommi, C., Romero, E., 2013. A fully coupled elastic-plastic hydromechanical model for compacted soils accounting for clay activity. Int. Journal for Numerical and Analytical Methods in Geomechanics 37, 503–535. http://dx.doi.org/10.1002/nag.1116.

Ellis, C. I. 1980. Soil compaction at low moisture content - field trials in sudan. Proceedings of the 7th Regional Conference for Africa on Soil Mechanics and Foundation Engineering, Accra, Ghana.

El Mountassir, G. 2011. *Behaviour of a collapsible, structured, unsaturated fill material*. PhD thesis, University of Strathclyde, Glasgow, UK.

Fredlund, D.G., Rahardjo, H., 1993. Soil Mechanics for Unsaturated Soils.Wiley, New York. xxiv, 517 pp.

Fookes, P.G., 1990. Tropical Residual Soils. Report of the Geological Society Engineering Group Working Party, Quarterly Journal of Engineering Geology; 23: 4–101.

Griffiths, F.J., and Joshi, R.C., 1989. Changes in pore size distribution due to consolidation of clays. Géotechnique, 39(1) :159-167.

Hidayat, F., Sungguh, H.M., Harianto, 2008. Impact of climate change on floods in Bengawan Solo and Brantas river basins, Indonesia. 11th International Riversymposium in Brisbane, Australia, 1 - 4 September 2008, published online at www.riversymposium.com.

Houston, S. and Houston, W. 1997. Collapsible Soil Engineering. Unsaturated Soil Engineering Practice, Geotech. Special Publication No. 68, ASCE, Houston and Fredlund, eds., 199 – 232.

Jommi, C., Sciotti, A., 2003. A study of the microstructure to assess the reliability of laboratory compacted soils as reference material for earth constructions. System-based vision for strategic and creative design, (Botempi, F. (ed)) vol 3. A.A. Balkema, Lisse, pp 2409–2415.

Lawton, E. C., Fragaszy, R. J., and Hardcastle, J. H. 1989. Collapse of compacted clayey soils. J Geotech Eng ASCE, 115: 1252-1267.

Lawton, E.C., Fragaszy, R.J., Hetherington, M.D. 1992. Review of wetting induced collapse in compacted soil. Journal of Geotechnical Engineering ASCE 118, 1376–1394.

Lee, P. Y. 1976. Study of irregular compaction curves. Soil Specimen Preparation for Laboratory Testing, ASTM STP 599, 278-288.

Lee, P. Y. and Suedkamp, R. J. 1972. Characteristics of irregularly shaped compaction curves. Highway Research Record, 381, 1-9.

Lloret, A., Villar, M. V., Sánchez, M., Gens, A., Pintado, X., and Alonso, E. E. 2003. Mechanical behaviour of heavily compacted bentonite under high suction changes. Géotechnique; 53(1): 2-40.

Mitchell, J.K., 1993. Fundamentals of soil behaviour, 2nd edn, Wiley.

Monroy, R., Zdravkovic, L. And Ridley, A. 2010. Evolution of microstructure in compacted London Clay during wetting and loading. *Géotechnique;* 60(2):105-119, doi:10.1680/geot.8.P.125.

Nawari, O. and Schetelig, K. 1991. Geotechnical study on kordofan tropical black soils (sudan republic).Eng Geol, 31, 1-26.

Olson, R. E. 1963. Effective stress theory of soil compaction. J Soil Mech Found Div ASCE,

89(SM2): 27-45.

Phien-weja, N., Pientonga, T. and Balasubramaniama, A.S., 1992. Collapse and strength characteristics of loess in Thailand. Engineering Geology; 32 (1-2): 59-72.

Poppe, L. J., Paskevich, V. F., and Hathaway, J. C., 2001. A laboratory manual for x-ray powder diffraction. Report, US Geological Survey Open-File Report 01-041.

Prapaharan, S., White, D.M., Altschaeffl, A.G., 1991. Fabric of field- and laboratory-compacted clay. Journal of Geotechnical Engineering ASCE 117 (12): 1934–1940.

Rao S. M. and Revanasiddappa, K. 2005. Role of microfabric in matrix suction of residual soils. Engineering Geology. 80: 60-70

Rao, S. M. and Revanasiddappa, K. 2003 Role of soil structure and matric suction on collapse of compacted soils. ASTM Geotechnical Testing Journal, 26: 102-110.

Romero, E. Gens, A. and Lloret, A., 1999. Water permeability, water retention and microstructure of unsaturated Boom clay. Engineering Geology, 54: 117-127.

Romero, E., Simms, P., 2008. Microstructure investigation in unsaturated soils: A review with special attention to contribution of mercury intrusion porosimetry and environmental scanning electron microscopy. Geotechnical and Geological

Engineering 26, 705-727.

Romero, E., Della Vecchia, G., and Jommi, C., 2011. An insight into the water retention properties of compacted clayey soils. Géotechnique, 61, 4, 313-328, doi: 10.1680/geot.2011.61.4.313

Romero, E. 2013. A microstructural insight into compacted clayey soils and their hydraulic properties, Engineering Geology, http://dx.doi.org/10.1016/j.enggeo.2013.05.024.

Sánchez, M., Gens A, Guimarães L, Olivella S., 2005. A double structure generalized plasticity model for expansive materials. International Journal for Numerical and Analytical Methods in Geomechanics, **29**:751-787.

Simms, P.H., and Yanful, E.K., 2001. Measurement and estimation of pore shrinkage and pore distribution in a clayey till during soil-water characteristic curve tests. Can. Geotech. J., 38: 741-754.

Soemitro, R., 2006. Personal communication.

Thom, R., Sivakumar, R., Sivakumar, V., Murray, E.J. and Mackinnon, P., 2007. Pore size distribution of unsaturated compacted kaolin: the initial states and final states following saturation. Géotechnique, 57(5): 469-474.

Table 1 Bengawan Solo fill soil properties

Properties	D1: 0.5 - 1.0m	D2: 1.0 – 1.5m
Particle density (Mg/m^3)	2.73	2.72
Sand content (%)	30	29
Silt content (%)	57	55
Clay content (%)	13	16
Uniformity Coefficient	29	27
Liquid Limit (%)	54	53
Plastic Limit (%)	36	37
Shrinkage Limit (%)	14	15
Plasticity Index (%)	18	16
Activity	1.4	1
Organic Content (%)	8	6
BSCS Classification	MHO	MHO

Table 2 Bengawan Solo soil mineralogy. Total fraction mineralogical semi-quantification by means of X-ray diffraction (% mass).

Minerals*	D1: 0.5 - 1.0m	D2: 1.0 -1.5m
Total Phyllosilicates	60	60
Quartz	18	14
Calcite	12	11
Plagioclases	9	14
Mg-hornblende	1	0.5

*Sample <63µm prepared

Table 3 Initial conditions of oedometer specimens

Series	Test Reference	Initial water content, w_o (%)	Initial dry density, ρ_{do} (Mg/m^3)	Relative Compaction, *RC* (%)	Loading Path
A	A1	20.8	1.17	80	Saturated at 3kPa → Loading
	A2	19.1	1.19	81	Unsaturated loading
	A3	20.8	1.17	80	Unsaturated loading to 32kPa → Wetting → Loading
	A4	18.2	1.16	79	Unsaturated loading to 63kPa → Wetting → Loading
	A5	18.8	1.15	78	Unsaturated loading to 125kPa → Wetting → Loading
	A6	20.5	1.16	79	Unsaturated loading to 253kPa → Wetting → Loading
	A7	20.5	1.19	81	Unsaturated loading to 538kPa → Wetting → Loading
B	B1	19.4	1.37	93	Saturated at 3kPa → Loading
	B2	19.4	1.37	93	Unsaturated loading
	B3	19.4	1.37	93	Unsaturated loading to 125kPa → Wetting → Loading
C	C1	29.2	1.44	98	Saturated at 3kPa → Loading
	C2	29.2	1.43	97	Unsaturated loading
	C3	29.2	1.43	97	Unsaturated loading to 125kPa → Wetting → Loading
D	D1	36.2	1.16	79	Saturated at 3kPa → Loading
	D2	35.4	1.20	82	Unsaturated loading
	D3	36.2	1.18	80	Unsaturated loading to 125kPa → Wetting → Loading
U	U1	33.6	1.23	84	Saturated at 3kPa → Loading
	U2	34.1	1.27	86	Unsaturated loading
	U3	35.6	1.23	84	Unsaturated loading to 63kPa → Wetting → Loading
	U4	35.7	1.12	76	Unsaturated loading to 125kPa → Wetting → Loading

Table 4 Initial conditions of specimens investigated in microstructural study

Specimen Name	Reference	w (%)	ρ_d (Mg/m^3)	e	S_r (%)
Compacted	A5-0	19.5	1.15	1.38	38.6
Compacted, loaded	A5-1	19	1.19	1.29	40.2
Compacted, loaded & collapsed	A5-2	27.7	1.39	0.95	79.2
Series D, Compacted	D	36.5	1.17	1.32	75.3
Undisturbed	U	34.7	1.36	1.00	94.4

List of Figures

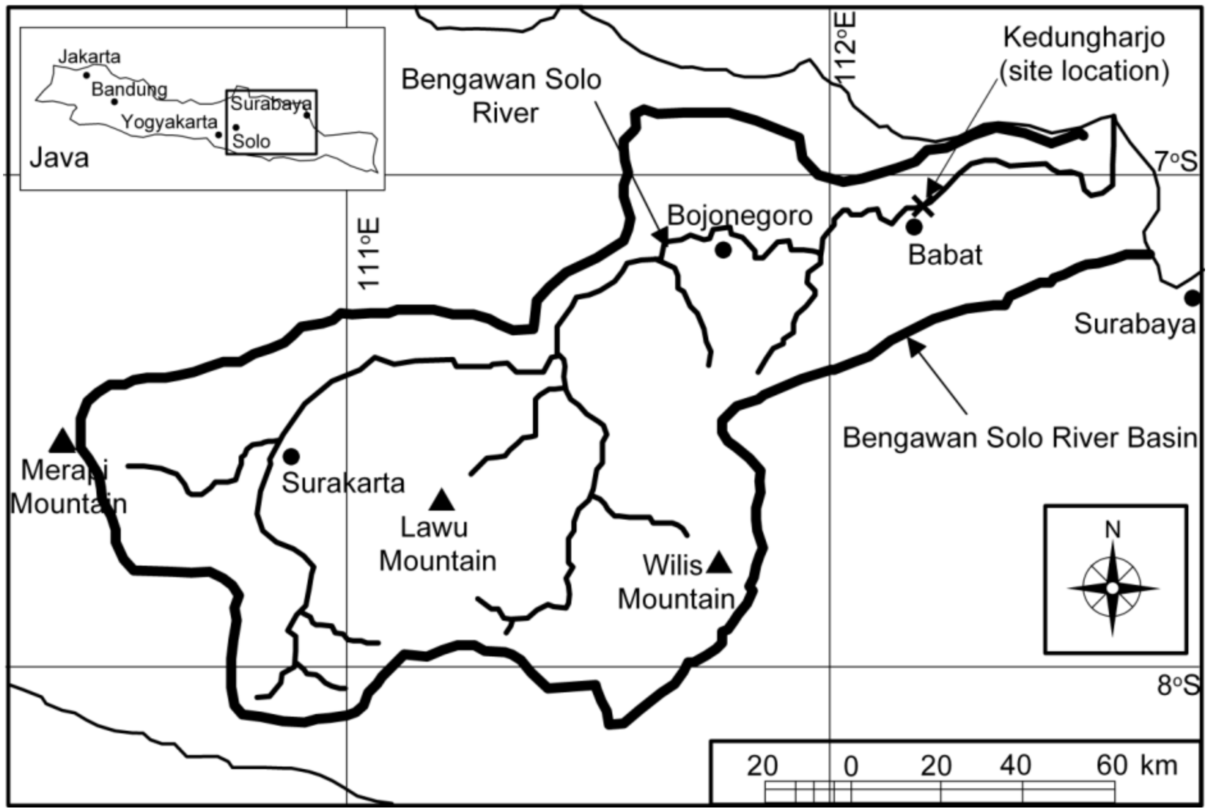

Figure 1. Location of the Kedungharjo site investigated along the Bengawan Solo River, East Java, Indonesia.

Figure 2. Two-step man-made embankment with surface protection in the form of rock filled gabions.

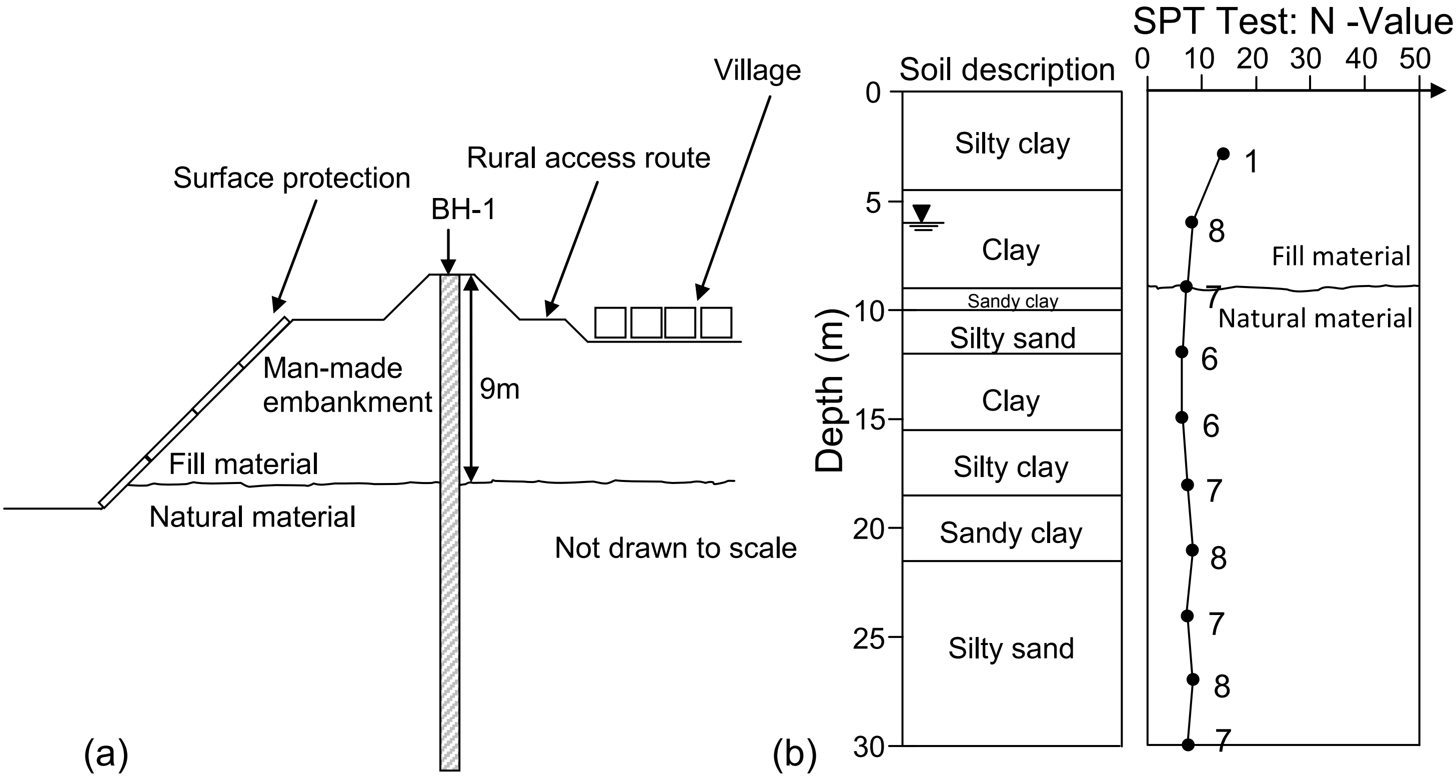

Figure 3. Man-made embankment at Kedungharjo (a) cross-section of embankment and (b) SPT profile.

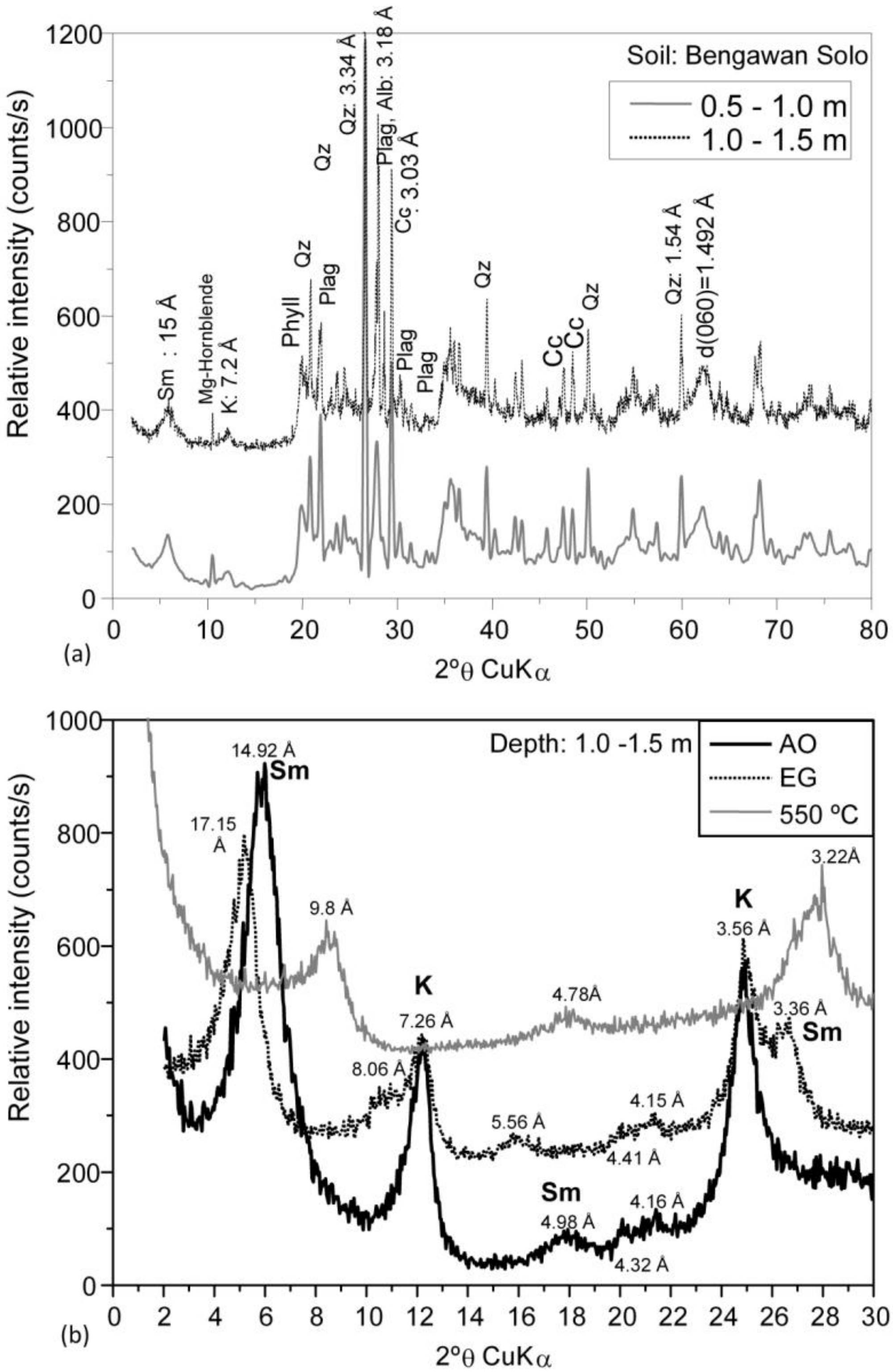

Figure 4. X-ray diffraction patterns of (a) random powder samples (< 63 μm) and (b) oriented samples (< 2μm fraction). Sm: montmorillonite, K: kaolinite, Phyll: total phyllosilicates, Qz: quartz, Plag: plagioclases; Cc: Calcite.

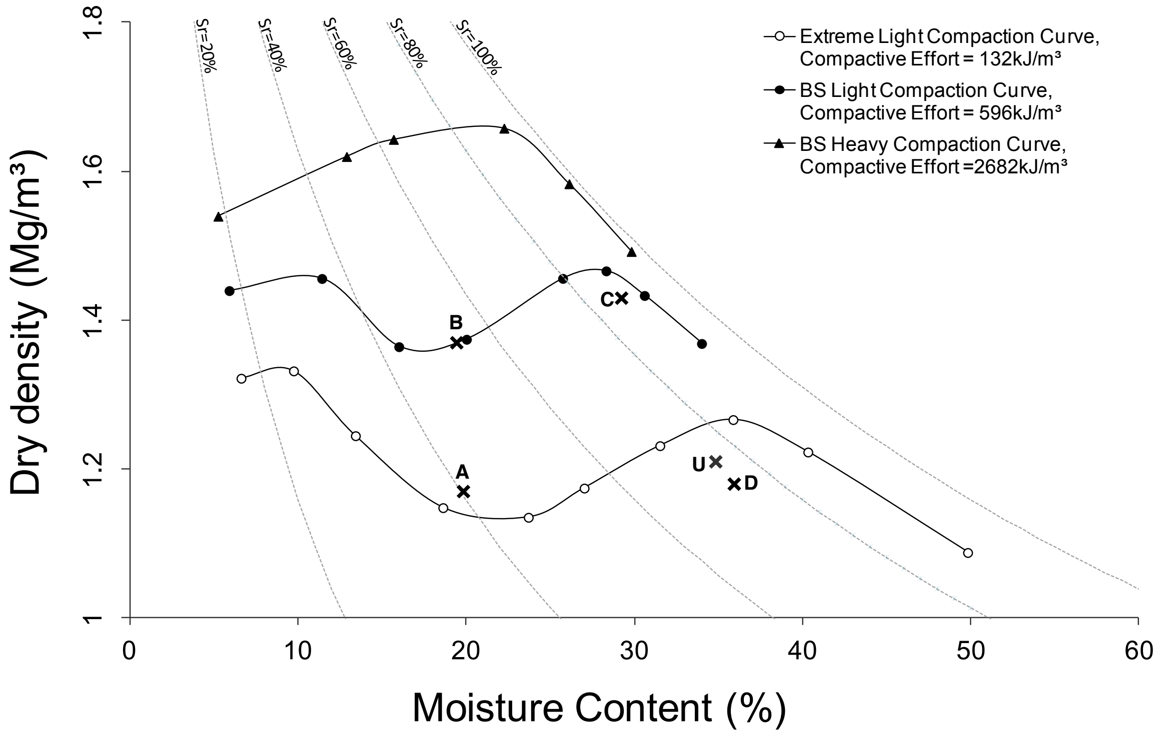

Figure 5. Compaction curves at three different energy levels (i) Extreme Light (132kJ/m3), (ii) BS Light (596kJ/m3) and (iii) BS Heavy (2682kJ/m3). Average initial conditions of Series A, B, C, D and U are also plotted.

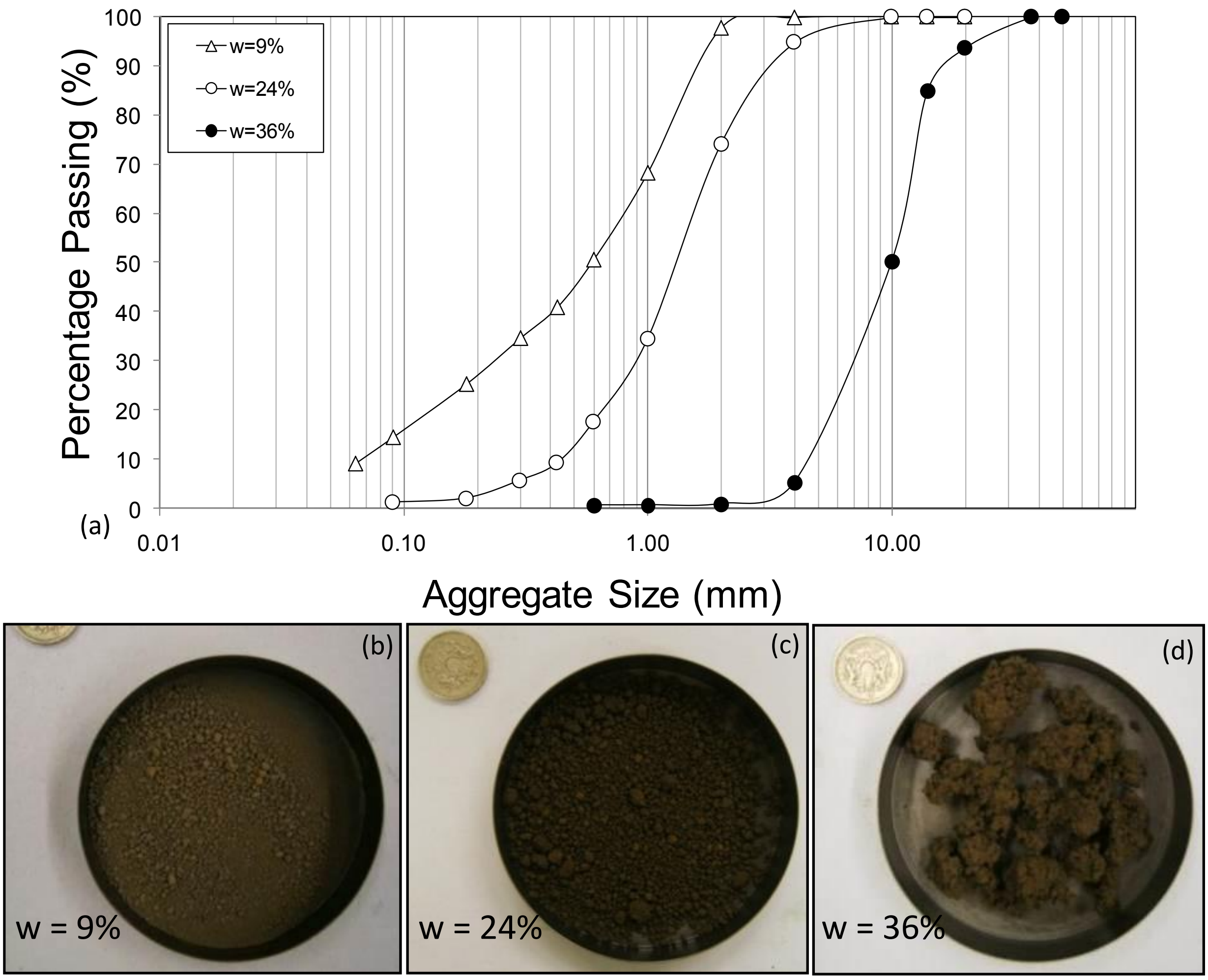

Figure 6. Influence of moisture content on aggregate size: (a) aggregate size distribution and (b, c, d) photographs of aggregates created.

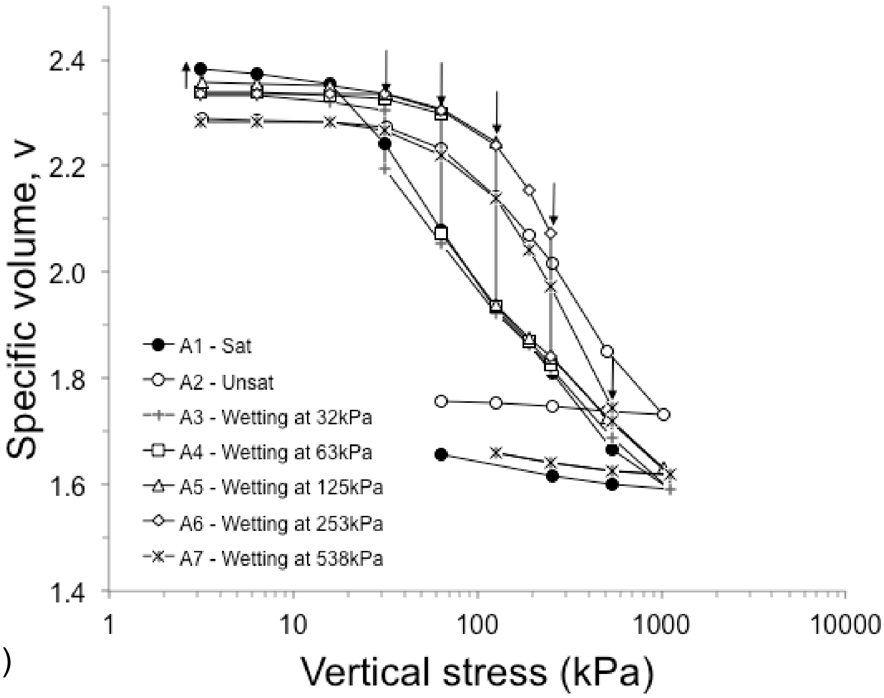

(a)

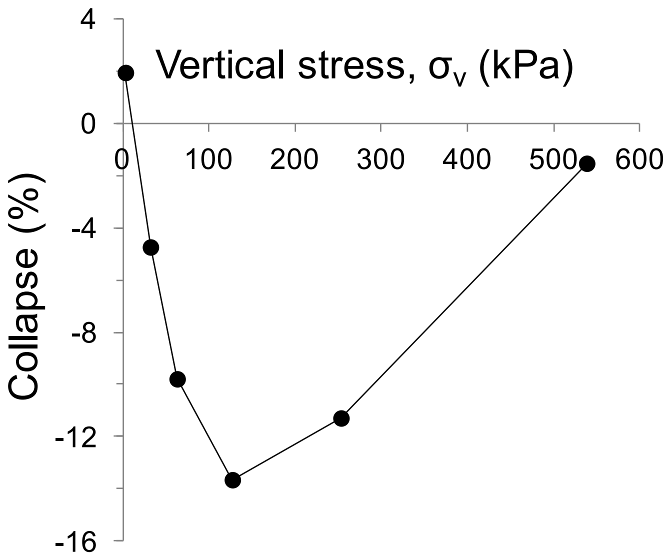

Figure 7. Oedometer Results: (a) Series A: Low density, dry of optimum samples, (b) Collapse potential at different vertical stresses for Series A.

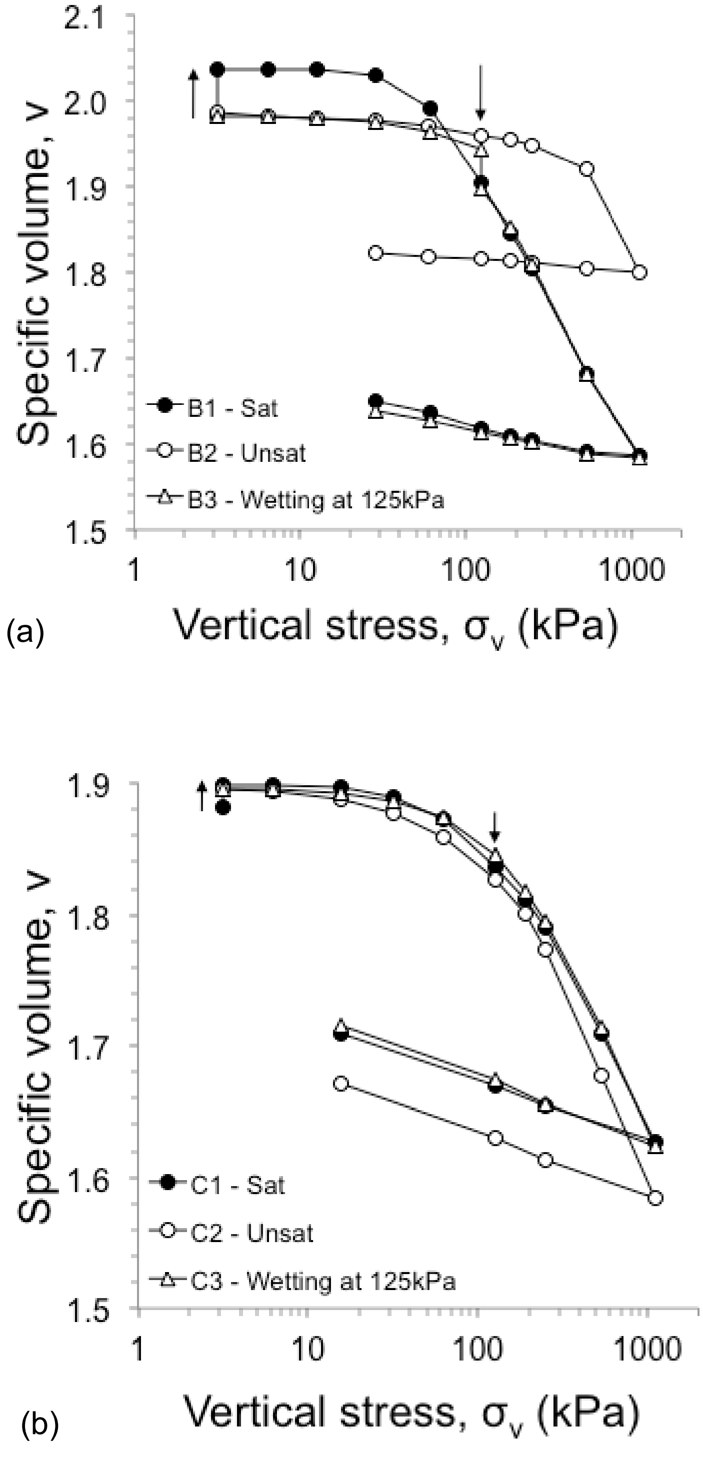

Figure 8. Oedometer Results: (a) Series B: High density, dry of optimum samples, (b) Series C: Close to BS Light optimum compaction conditions.

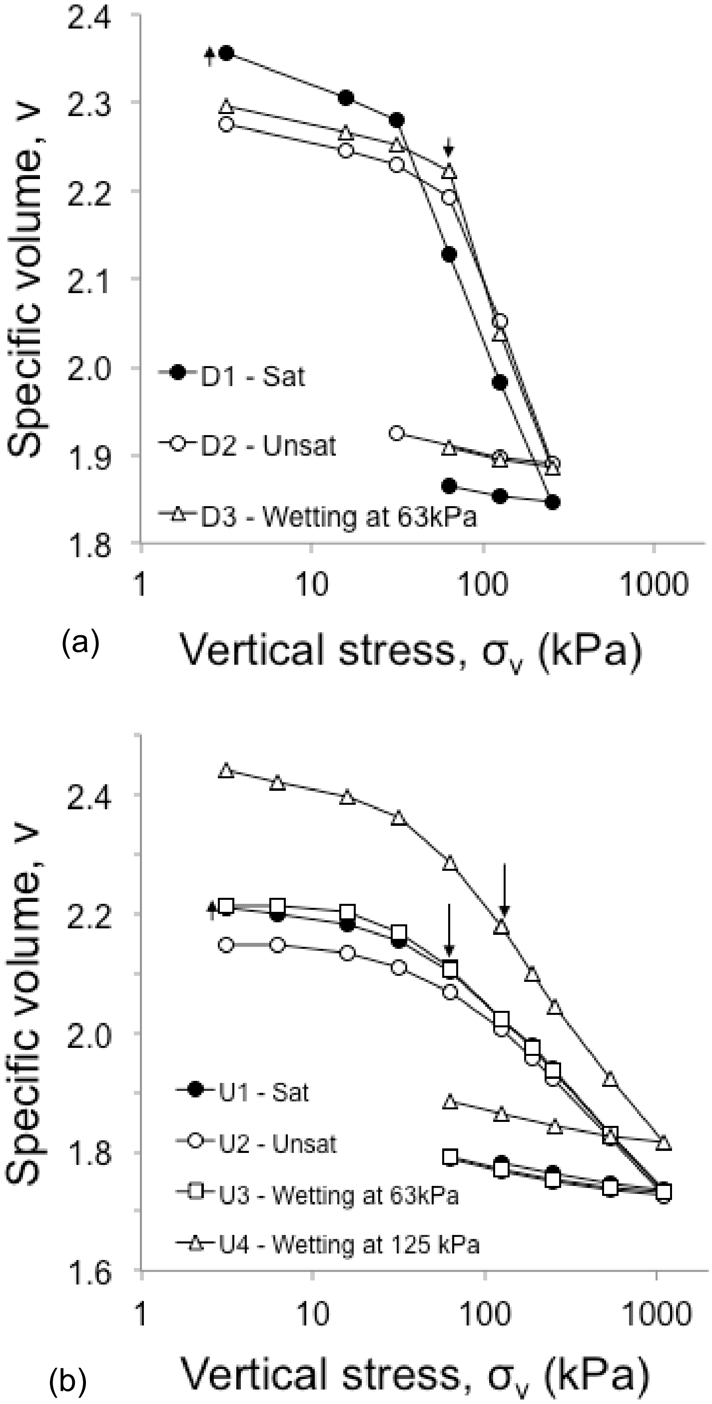

Figure 9. Oedometer Results: (a) Series D: Optimum w% of Extreme Light compaction curve at low dry density, (b) Series U: Undisturbed specimens.

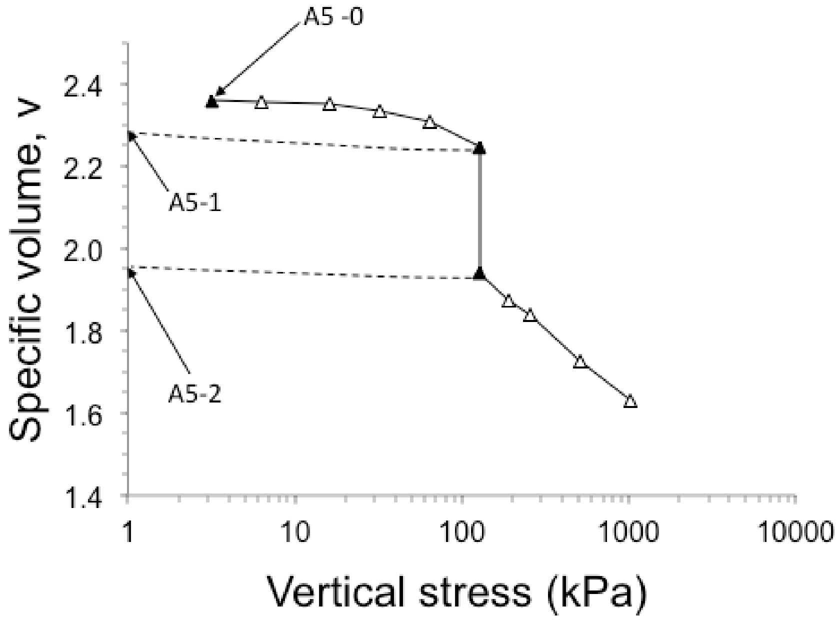

Figure 10. Specimens selected for investigation in fabric study according to load and soak tests: (i) A5-0 Compacted, (ii) A5-1 - Compacted loaded and (iii) A5-2 - Compacted loaded & collapsed.

Figures 11 and 12
Click here to download Figure: Figures-rev 11 to 12.doc

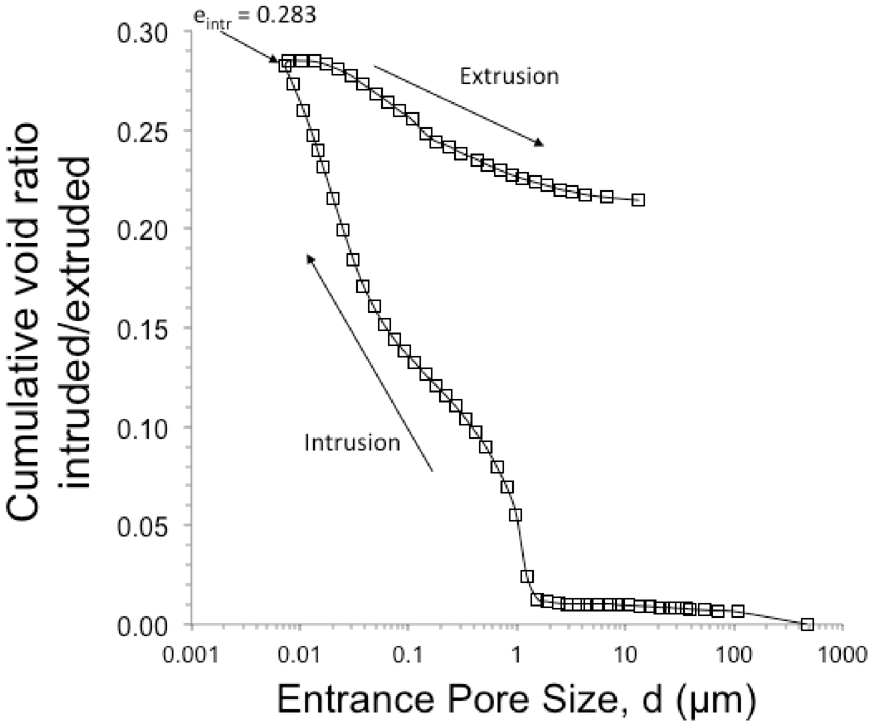

Figure 11. MIP results of high density dried slurry specimen in terms of cumulative void ratio intruded.

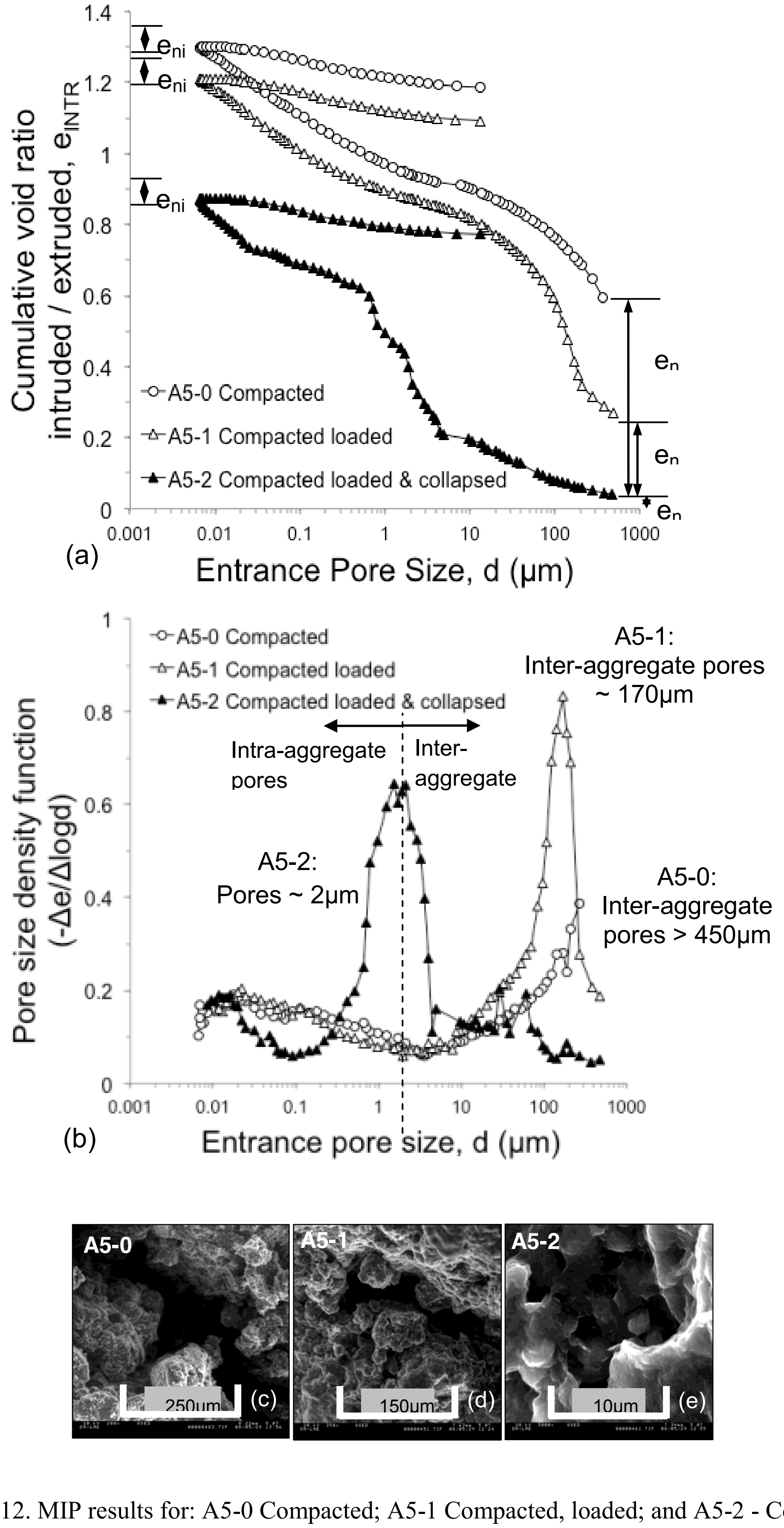

Figure 12. MIP results for: A5-0 Compacted; A5-1 Compacted, loaded; and A5-2 - Compacted, loaded & collapsed specimens. (a) Cumulative void ratio intruded. (b) Pore size density function. Void ratio non-intruded e_{ni}= 0.078 for all specimens. Void ratio non-detected, A5-0: e_{nd}= 0.568, A5-1: e_{nd} = 0.269, A5-2: e_{nd} = 0.050. Evidence of corresponding dominant pore sizes are illustrated in (c), (d) and (e).

Figure 13
Click here to download Figure: Figures-rev 13.doc

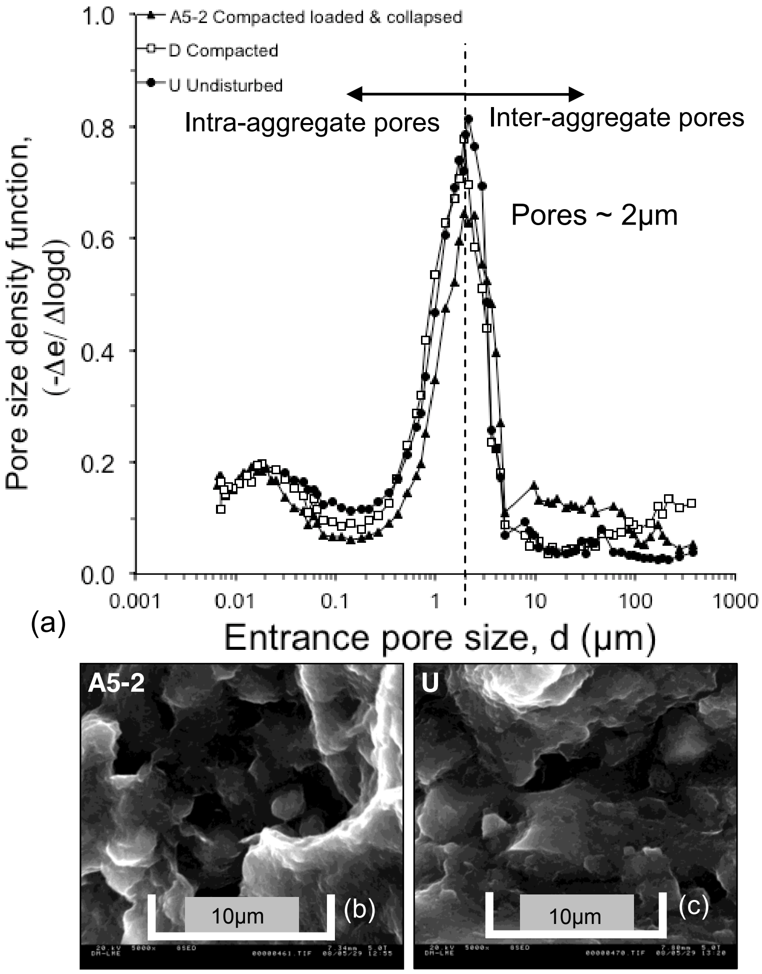

Figure 13. Pore size density function plots for (i) A5-2 Compacted loaded &collapsed, (ii) D - Series D Compacted and (iii) Undisturbed samples. Evidence of corresponding dominant pore sizes are illustrated in (b) and (c).

Figures 14 to 16
Click here to download Figure: Figures-rev 14 to 16.doc

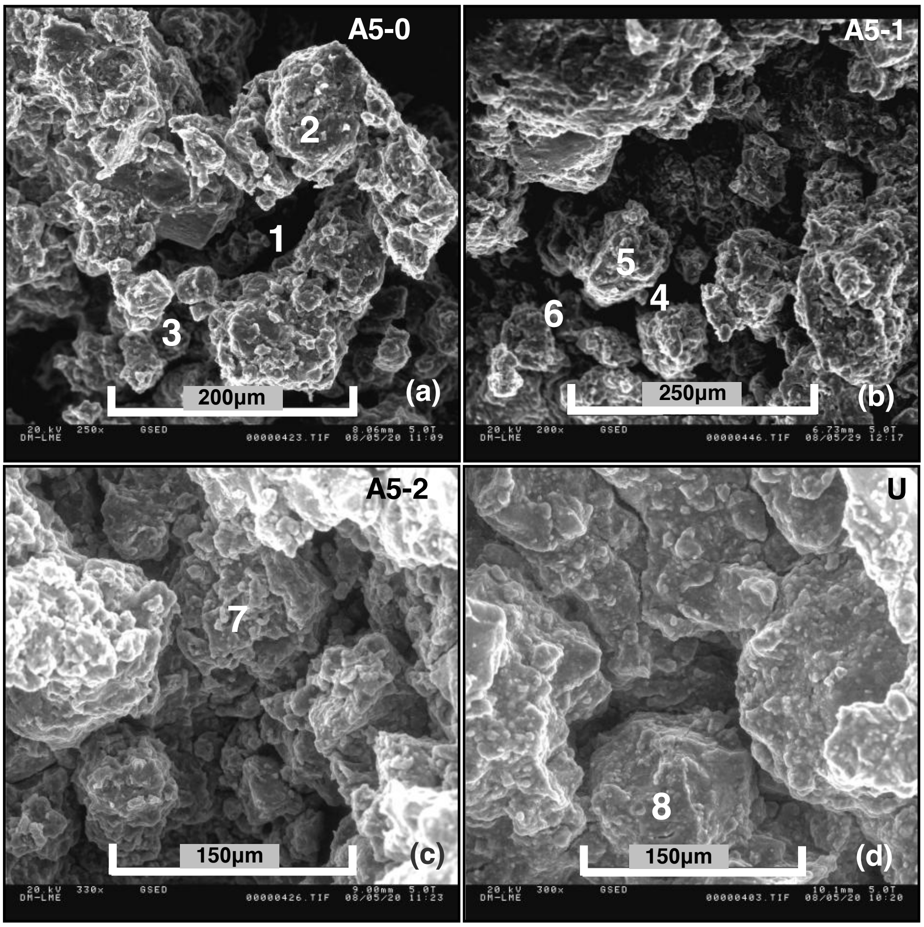

Figure 14. ESEM micrographs of: (a) A5-0 Compacted, (b) A5-1 Compacted, Loaded (c) A5-2 Compacted, Loaded & Collapsed and (d) U - Undisturbed specimen.

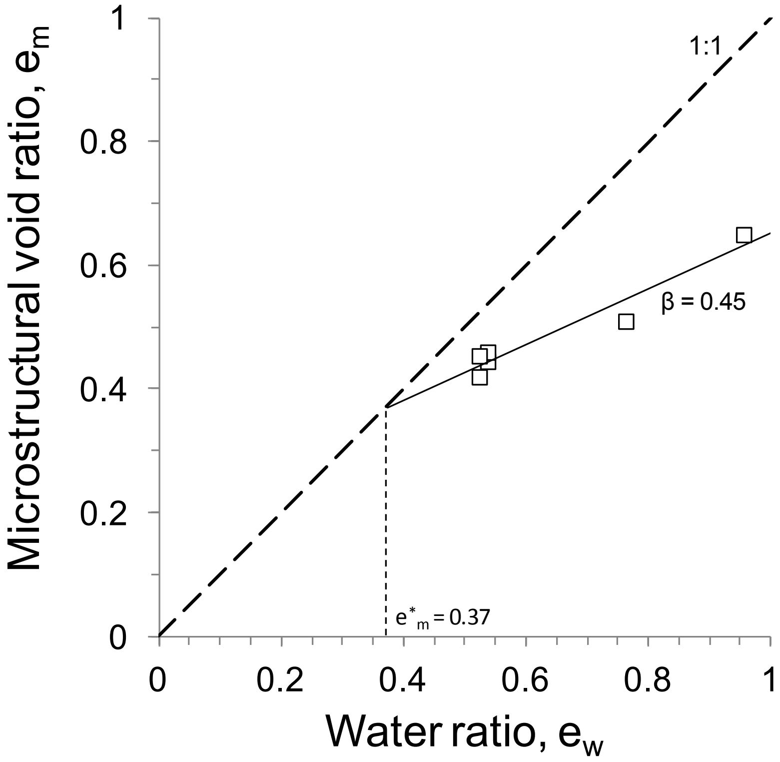

Figure 15. Evolution of microstructural void ratio with water ratio from MIP results for the Bengawan Solo fill

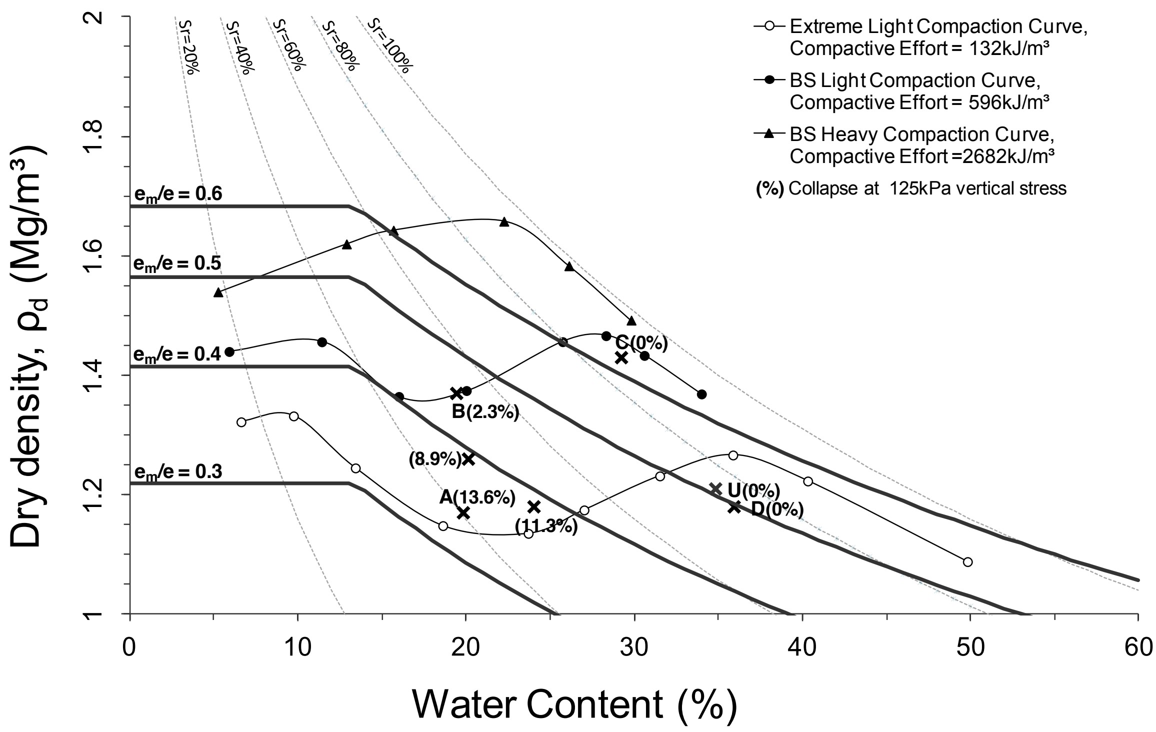

Figure 16. Contours of constant e_m/e for the Bengawan Solo fill plotted on the compaction plane (water content versus dry density).